

# The band gap variation of a two dimensional binary locally resonant structure in thermal environment

Cite as: AIP Advances 7, 015002 (2017); <https://doi.org/10.1063/1.4973723>

Submitted: 20 September 2016 • Accepted: 24 December 2016 • Published Online: 03 January 2017

Zhen Li, Xian Wang and  Yue-ming Li



View Online



Export Citation



CrossMark

## ARTICLES YOU MAY BE INTERESTED IN

[Thermal stress effects on the flexural wave bandgap of a two-dimensional locally resonant acoustic metamaterial](#)

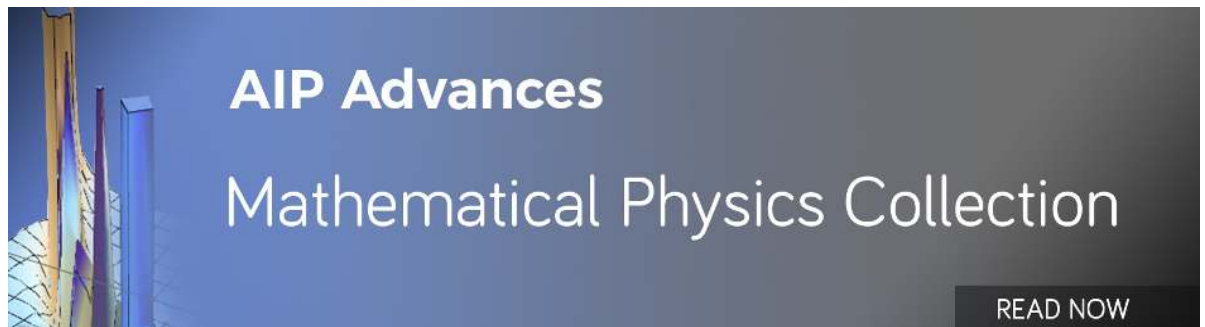
Journal of Applied Physics **123**, 195101 (2018); <https://doi.org/10.1063/1.5019862>

[Thermal tuning of negative effective mass density in a two-dimensional acoustic metamaterial with hexagonal lattice](#)

Journal of Applied Physics **126**, 155102 (2019); <https://doi.org/10.1063/1.5109597>

[The Lamb wave bandgap variation of a locally resonant phononic crystal subjected to thermal deformation](#)

AIP Advances **8**, 055109 (2018); <https://doi.org/10.1063/1.5026523>



## The band gap variation of a two dimensional binary locally resonant structure in thermal environment

Zhen Li, Xian Wang, and Yue-ming Li<sup>a</sup>

*State Key Laboratory for Strength and Vibration of Mechanical Structures, Shaanxi Key Laboratory of Environment and Control for Flight Vehicle, School of Aerospace, Xi'an Jiaotong University, Xi'an 710049, China*

(Received 20 September 2016; accepted 24 December 2016; published online 3 January 2017)

In this study, the numerical investigation of thermal effect on band gap dynamical characteristic for a two-dimensional binary structure composed of aluminum plate periodically filled with nitrile rubber cylinder is presented. Initially, the band gap of the binary structure variation trend with increasing temperature is studied by taking the softening effect of thermal stress into account. A breakthrough is made which found the band gap being narrower and shifting to lower frequency in thermal environment. The complete band gap which in higher frequency is more sensitive to temperature that it disappears with temperature increasing. Then some new transformed models are created by changing the height of nitrile rubber cylinder from 1mm to 7mm. Simulations show that transformed model can produce a wider band gap (either flexure or complete band gap). A proper forbidden gap of elastic wave can be utilized in thermal environment although both flexure and complete band gaps become narrower with temperature. Besides that, there is a zero-frequency flat band appearing in the first flexure band, and it becomes broader with temperature increasing. The band gap width decreases trend in thermal environment, as well as the wider band gap induced by the transformed model with higher nitrile rubber cylinder is useful for the design and application of phononic crystal structures in thermal environment. © 2017 Author(s). All article content, except where otherwise noted, is licensed under a Creative Commons Attribution (CC BY) license (<http://creativecommons.org/licenses/by/4.0/>). [<http://dx.doi.org/10.1063/1.4973723>]

### I. INTRODUCTION

The unique characteristic of band gap in periodic structures or phononic crystals has attracted great attention,<sup>1-5</sup> because it provides a new solution for reducing vibration and noise in machinery, aerospace, architecture, transportation and other fields. Since the locally resonant phononic crystal (in short PC) was proposed in 1993, the band gap frequencies had reduced at least one or two orders of magnitude lower than that produced by the Bragg scattering mechanism.<sup>1</sup> M. Oudich<sup>6-8</sup> studied the locally resonant sonic band gap by using one side and double-sides stubbed PC plate. It was obtained that the band gap was various with the change of pillars' height and radius. P. Wang et al.<sup>14</sup> investigated the evolution of band gaps in the double-sided PC plate by adjusting the height of stub. They found that when the double stubs arranged symmetrically on both sides, new bands appeared and the bands became more flat. About the binary structure, J. C. Hsu<sup>9,10</sup> studied the lamb waves in a cylinder binary plate with two dimensional lattices. They reached that the thickness of plate and the radius of soft rubber pillars had an obvious influence in the band gap. Generally, there are abundant researches about how to create a new band gap in previous work. What is worth mentioning is to take thermal effect into account when PC structures serve in thermal environment, since the impact of thermal load on the dynamic characteristic and noise reduction properties of structure cannot be neglected.<sup>10-13</sup>

---

<sup>a</sup>Author to whom correspondence should be addressed. Electronic mail: [liyueming@mail.xjtu.edu.cn](mailto:liyueming@mail.xjtu.edu.cn)

Recently, it starts to receive increasing attention that temperature variation may lead to the shift in PC band structure. For beginning, a number of studies were focused on the material properties which are sensitive to temperature such as the longitudinal (transverse) sound velocity, the Young's modulus et al.<sup>18,19</sup> Besides that, Yao et al.<sup>15</sup> found that the effect of thermal load on band gap is related to lattice form and material components by computing two dimensional PC plate though supercell-plane-wave-expansion-method. They concluded that thermal can tune the band gap but didn't describe the thermal effect qualitatively and quantitatively.

In this study, with the consideration of thermal stress, we present the numerical investigation of thermal effect on PC structure, which is composed of nitrile rubber cylinder periodically filling in aluminum plate. Based on the binary structure studied by Hsu et al.,<sup>10</sup> firstly, we research the band gap variation trend under the influence of initial thermal stress. As a result, the flexure band gap becomes narrower under thermal environment and the complete band gap is more sensitive to temperature that it disappears with temperature increasing. To obtain a proper forbidden band under thermal, then we create a new model which transform the height of rubber cylinder from 3 to 7mm progressively. The soft rubber cylinder is distributed symmetrically in the drilled aluminum plate. Corresponding band structures of the new models show that the band gaps are enlarged as expect. With the increasing of height, the flexure gap disappears gradually. Meanwhile the complete gap emerges. There are still apparent forbidden band though both flexure and complete band gaps are narrower under temperature of 70°C. Meanwhile, a new phenomenon is detected that a zero-frequency flat band appears in the first flexure band along with the imposing of thermal stress. The band gap width decreases trend in temperature and the wider band gap induced by the transformed model can be useful for the PC structures serving in thermal environment.

## II. MODEL AND COMPUTATION THEORY

The PC structure is comprised of aluminum plate filled with nitrile rubber cylinder periodically. FIG. 1 shows the unit cell that the height of nitrile rubber cylinder  $h=1\text{mm}$ , the lattice constant  $a=10\text{mm}$ , the radius of nitrile rubber  $r=4\text{mm}$ . About material parameters, the material Young modulus, density, Poisson's ratio and thermal expansion coefficient are listed below. The subscripts A and R are for aluminum and rubber respectively.

Aluminum:  $E_A = 77.6\text{GPa}$ ,  $\rho_A = 2730\text{kg/m}^3$ ,  $\mu_A = 0.352$ ,  $\alpha_A = 2.32 \times 10^{-5}/\text{K}$

Nitrile rubber:  $E_R = 1.2 \times 10^{-2}\text{GPa}$ ,  $\rho_R = 1300\text{kg/m}^3$ ,  $\mu_R = 0.47$ ,  $\alpha_R = 1.96 \times 10^{-4}/\text{K}$

FIG. 2 shows the transformed model which the height of nitrile rubber is changed and the height  $h=3, 5, 7\text{mm}$  are studied respectively. The soft rubber cylinder is filled in aluminum plate and distributed symmetrically along z-axis direction in the drilled aluminum plate.

Finite element method is one of the effective ways to compute the band structure of PC with complex topology. In this paper, all the numerical analysis are implemented by using finite element software Comsol Multiphysics. Since the PC structure is formed by a periodic array of unit cells, only one cell is considered in our computation. Therefore the periodic boundary conditions are used for the interfaces between the nearest unit cells. According to the Bloch theorem, the displacement fields of the unit cell obey the equation (1) as the follow condition:<sup>10</sup>

$$u_i(x + a, y + a) = u_i(x, y) \exp(ik_x a + ik_y a) \quad (1)$$

where  $k_x$  and  $k_y$  are the components of the Bloch wave vectors in the x and y directions respectively.

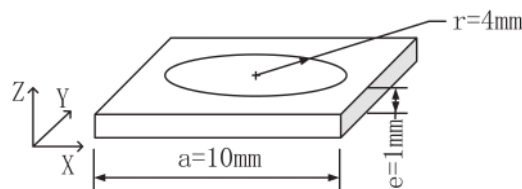


FIG. 1. Geometry parameters of the unit cell.

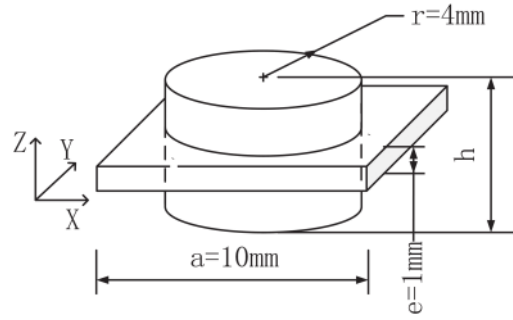


FIG. 2. The unit cell with different height of nitrile rubber cylinder.

The band structure computation with temperature is different from the usual and can be separated to two steps. In the first step, a static analysis is applied to compute the interior thermal stress of the unit cell. In this study, we are focusing on the thermal stress affecting the band structure of PC, and all the material's behavior is set as the liner elastic for simplicity. Here a spring support is imposed on one point of the cell in order to limit the rigid body displacement but does not constrain the thermal deformation as well not change the eigen frequency of the unit. The spring support together with the periodic boundaries is applied to the cell in both steps. In step two, the thermal stress components are imposed to the unit cell as an initial stress. The imposed stress is not initial values in the mathematical sense, but rather a contribution to the constitutive relation. Then a regular band structure computation is conducted.

When the structure suffers from the thermal, it will induce a reduction in stiffness which is reflected in material's properties variation and thermal stress.<sup>16</sup> Furthermore, in terms of the macrostructure, when the body is subjected to external loads, the real deformation and stress fields show large gradients because of the heterogeneities.<sup>20</sup> Those factors may result in multiple affects to the structure. Here, only the thermal stress is taken into account. Based on the classical theory of liner thermoelasticity, the components of the strain tensor due to the temperature change can be written as equation (2),<sup>22</sup> which the thermal strain is introduced following the equation (3):<sup>21</sup>

$$\boldsymbol{\varepsilon}_{ij} = \boldsymbol{\varepsilon}_{ij}^e + \boldsymbol{\varepsilon}_{ij}^{th} \quad (2)$$

$$\boldsymbol{\varepsilon}_{ij}^{th} = [\varepsilon_x \ \varepsilon_y \ \varepsilon_z \ \gamma_{xy} \ \gamma_{yz} \ \gamma_{xz}]_{th}^T = \alpha(T - T_{ref})\boldsymbol{\delta}_{ij} \quad (3)$$

where  $\boldsymbol{\varepsilon}_{ij}^e$  denotes the elastic strain and  $\boldsymbol{\varepsilon}_{ij}^{th}$  stands for the thermal strain,  $T$  is the actual temperature, and  $T_{ref}$  is the reference temperature,  $\alpha$  is the coefficient of thermal expansion,  $\boldsymbol{\delta}_{ij}$  is Kronecker delta.

According to the stress-strain relations from Hooke's law, the stress expression can be obtained from equation (2). The in-plane stress tensor is expressed in equation (4):<sup>22</sup>

$$\boldsymbol{\sigma}_{ij} = \frac{E}{1 - \mu^2} \left[ \mathbf{D}\boldsymbol{\varepsilon}_{ij}^e - \alpha(1 + \mu)(T - T_{ref})\boldsymbol{\delta}_{ij} \right] \quad (4)$$

where  $\mu$  is the Poisson's ratio of material,  $\mathbf{D}$  is denoted as  $\begin{bmatrix} 1 & \mu & 0 \\ \mu & 1 & 0 \\ 0 & 0 & \frac{1-\mu}{2} \end{bmatrix}$ .

Considering that the thickness of PC plate is much less than its size in-plane. Further, the structure expansion along  $z$ -axis will not induce thermal stress in uniform temperature fields for its free boundary condition, so that the thermoelasticity problem of PC plate can be regarded as the

plane stress state. The stress-displacement relations obey the equation (5):<sup>22</sup>

$$\begin{aligned}\sigma_x &= \frac{E}{1-\mu^2} \left[ \left( \frac{\partial u}{\partial x} + \mu \frac{\partial v}{\partial y} \right) - \alpha(1+\mu)(T-T_{ref}) \right] \\ \sigma_y &= \frac{E}{1-\mu^2} \left[ \left( \frac{\partial v}{\partial y} + \mu \frac{\partial u}{\partial x} \right) - \alpha(1+\mu)(T-T_{ref}) \right] \\ \sigma_{xy} &= \frac{E}{2(1+\mu)} \left( \frac{\partial u}{\partial y} + \frac{\partial v}{\partial x} \right)\end{aligned}\quad (5)$$

where  $u$  and  $v$  are the in-plane displacement components caused by temperate variation,  $E$  and  $\mu$  are the young's modulus and the Poisson's ratio of two materials respectively.

Theoretically, there are two reasons inducing the thermal stress: on the one hand, the thermal stress will produce in-plane by the result of the different thermal expansion coefficient of two materials. On the other hand, in view of homogenization theory, two joined cells must still fit together in their common deformed state. In mechanical terms, this means that when passing from a cell to the next one, the stress vector is continuous together with the strains are compatible.<sup>20</sup> The identical deformation among the nearest cells may also lead to the thermal stress when temperature is changed. This statement is supported by that stress state of the periodic boundary condition is the same as the in-plane displacement constraint situation in Comsol static analysis.

Based on the applying of periodic conditions, the in-plane displacement of the unit cell is constraint by the surrounding cells in infinite PC plate. Here the stress can be simplified as equation (6):

$$\begin{aligned}\sigma_x &= -\frac{E\alpha(T-T_{ref})}{1-\mu} \\ \sigma_y &= -\frac{E\alpha(T-T_{ref})}{1-\mu} \\ \sigma_{xy} &= 0\end{aligned}\quad (6)$$

Integral equation (6) along the thickness of PC plate, the in-plane stress of per unit area can be obtained, which is known as the membrane force as equation (7) shows:

$$\begin{aligned}N_x &= -\frac{E\alpha h(T-T_{ref})}{1-\mu} \\ N_y &= -\frac{E\alpha h(T-T_{ref})}{1-\mu} \\ N_{xy} &= 0\end{aligned}\quad (7)$$

where  $h$  is the thickness of plate.

As a consequence, the  $\sigma_x$ ,  $\sigma_y$ ,  $\sigma_{xy}$  of two models are presented in FIG. 3. By a comparison among the six thermal stress components, it is verified that  $\sigma_z$ ,  $\sigma_{xz}$ ,  $\sigma_{yz}$  are much smaller than in-plane stress and those maximums even no more than three percent of the peaks of  $\sigma_x$  together with  $\sigma_y$ . That means the equivalent of converting the PC plate analysis to the plane-stress state is reasonable. Note that the normal stress along x, y directions is larger than the  $\sigma_{xy}$  component and is dominant in thermal stress components. Simultaneously, there is an interesting phenomenon that two pairs of tension and compressive stresses occur in the interface of two materials in shear stress contour, though most area's stress is nearly to zero. The reason is that the shear strain caused by different thermal expansion appearing in the junction of two materials, while it equals to zero in isotropic material. Obviously, the height of nitrile rubber has almost no effect in the distribution of in-plane stress.

The membrane forces which are induced by temperature variation can be obtained by static analysis. Then the thermal stress matrix will be defined for plate model as equation (8) as follow:<sup>17</sup>

$$[\mathbf{K}_\sigma] = \sum_i \int_{A_i} [\mathbf{G}]^T \begin{bmatrix} N_x & N_{xy} \\ N_{xy} & N_y \end{bmatrix} [\mathbf{G}] dA \quad (8)$$

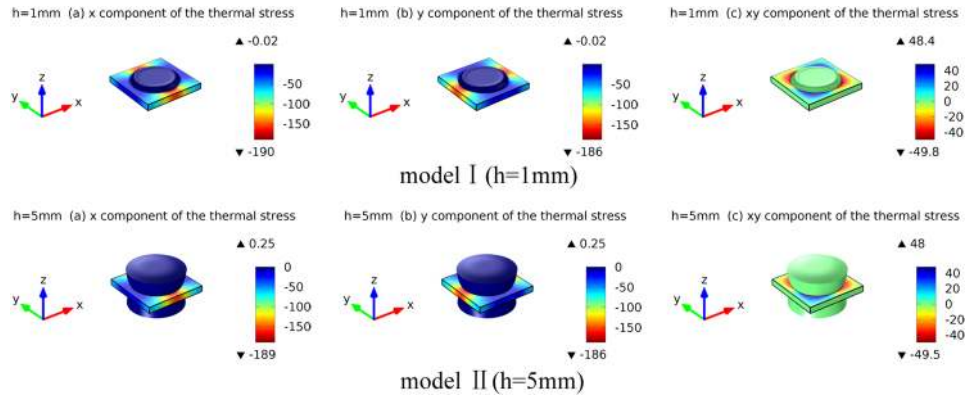


FIG. 3. The thermal stress distribution of two models in 70°C(unit: MPa).

where  $[\mathbf{K}_\sigma]$  is the stress stiffness matrix produced by thermal stress,  $[\mathbf{G}]$  is the strain-displacement matrix,  $N_x$ ,  $N_y$  and  $N_{xy}$  are the static membrane forces respectively, and  $A_i$  is the area of the  $i_{th}$  element.

After that, the thermal stress components are added as an initial stress to the eigen frequency analysis in step two. Consequently the dynamic stiffness matrix of structure with membrane forces can be expressed as equation (9):<sup>17</sup>

$$([\mathbf{K} + \mathbf{K}_\sigma] - \omega^2 [\mathbf{M}]) \{\mathbf{U}\} = \{0\} \quad (9)$$

where  $[\mathbf{K}]$  is the conventional stiffness matrix,  $\omega$  is the angular frequency,  $[\mathbf{M}]$  is the mass matrix,  $\{\mathbf{U}\}$  is the amplitude vector of nodal degree of freedom.

Here it is necessary to note that the effect of the additional stress matrix varies from different stress state. When the stress is in tensile state, it turns to positive and enlarges the structure stiffness. When the stress state is compressive, the additional matrix changes to soften the original stiffness. It is obvious that the thermal stress is in compressive state for the present problem and it takes a side-effect on the structures stiffness, which makes the frequencies shift to lower region. For the PC structure, it causes a drift of band gaps.

In our computation, the thermal expansion coefficients are treated as constants because the temperature is not too high. And the reference temperature is 293.15K, for it is close to the room temperature, in which the thermal stress is zero. As for the mesh generation, the free quadrangle mesh is chosen in the upper surface of the model. Then the sweep operation is taken to mesh the whole geometry. The finer size is chosen so as to maintain a balance between the computation accuracy and work time.

### III. NUMERICAL RESULTS AND ANALYSIS

In analyzing the thermal influence in band gap, band structure of the cell in changing temperature is computed. FIG. 4 shows the band structure of unit cell in room temperature. There are two obvious gaps, in which the frequency range from 2817.3 to 3104.5Hz is a flexure band gap, and the frequency range from 8405 to 8771.2 is a complete bandgap. FIG. 5 shows the flexure modal of point A and point B, and the vibration modal of point C and point D of the corresponding point shown in FIG. 4. The locally resonant modal in flat band illustrates that natural frequency is equal in all direction. Note that the vibration displacement of the cell is mainly focused in nitrile rubber when it is in locally resonant modal. Consequently, the vibration will be limited in the elastic stubs?? when the frequency is during the gaps.

Furthermore, we research the variation trend of band structure in thermal environment. The changes of band gaps with temperature are plotted in FIG. 6. Computation results show that both the complete band gap and the flexure band gap become narrower with temperature. It can be found that the start and stop frequency of both gaps drift to lower frequency as temperature increase. Note that the complete band gap which at higher frequency is more sensitive to thermal that it disappears at

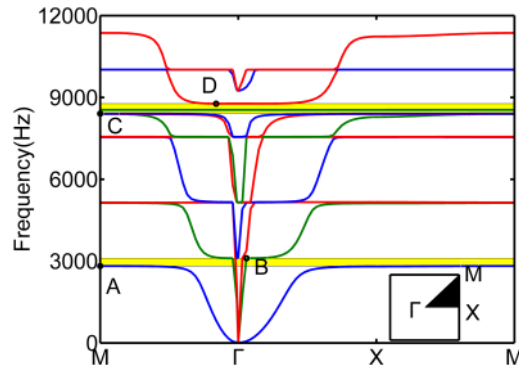


FIG. 4. Band structure of two dimensional binary unit cell at room temperature.

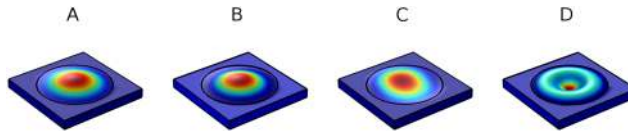


FIG. 5. The vibration modal of the corresponding point (A, B, C, D) denoted in FIG. 4.

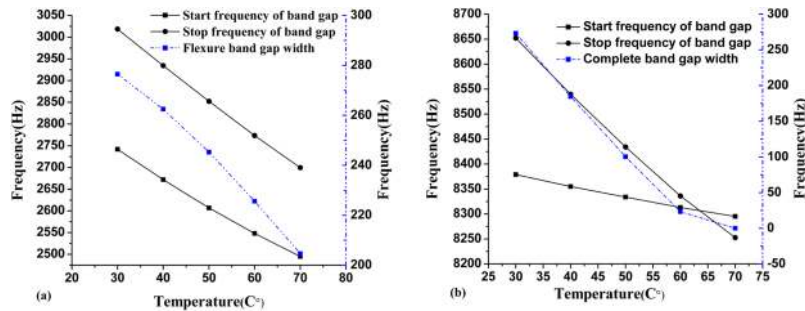


FIG. 6. Flexure and complete band gap variation trend with temperature.

70°C. Those simulation results mean that the thermal stress of components should be considered in design, for the temperature variation has a deep impact on both the flexure and complete band gaps.

To obtain proper forbidden gap of elastic wave in thermal environment, we alter the height of rubber cylinder. FIG. 7, FIG. 8, and FIG. 11 show the corresponding band structures of  $h=3, 5, 7$  mm respectively. It can be seen that band gaps are different from various nitrile rubber cylinder height. Apparently, the band gaps (either flexure or complete band gap) of transformed model are wider than which induced by initial model. Besides that, the flexure gap disappears gradually and the complete gap emerges.

With considering of thermal stress, all the bands are shifted to lower frequency in FIG. 7(b), FIG. 8(b), and FIG. 11(b). Even though flexure or complete band gaps of the binary cell become narrower under thermal environment, these band gaps are still available for the structure's vibration and noise reduction at the temperature of 70°C. To have a direct view of the created model's vibration, the modals of point A, B, C, D which marked on the band structure of 5mm are shown in FIG. 9. It is obvious that the vibration mainly focuses on soft rubber. With the height of rubber cylinder increasing, the wider band gap induced by the transformed model can overwhelm the softening impact of thermal stress. Therefore, a proper band gap will appear in thermal environment.

It is notable that there is a wide range of wave vector near the  $\Gamma$  point corresponding to zero frequency in the lowest flexure band in temperature of 70°C in FIG. 7(b), FIG. 8(b), and FIG. 11(b). To understand this new phenomenon, we present the evolution of the zero-frequency flat band with temperature of 30°C and 50°C in FIG. 10. (a) and (b). The calculation object is the transformed



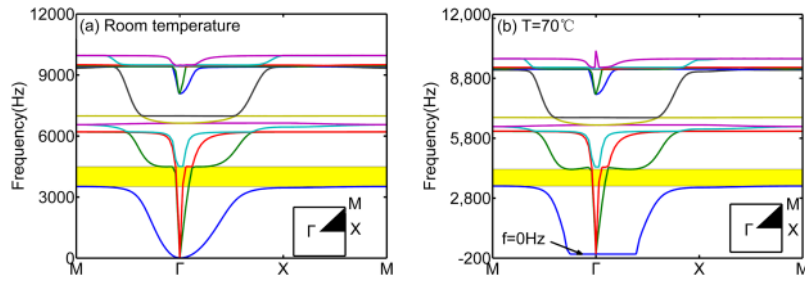
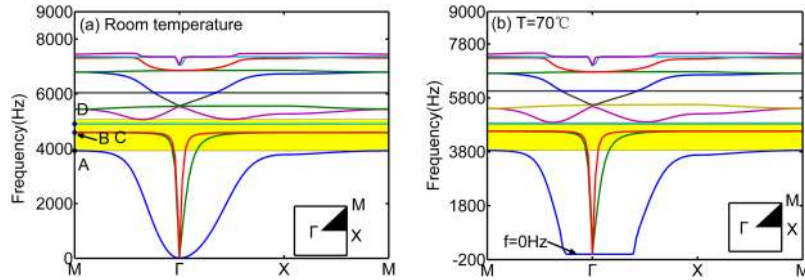
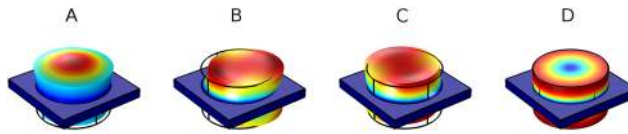
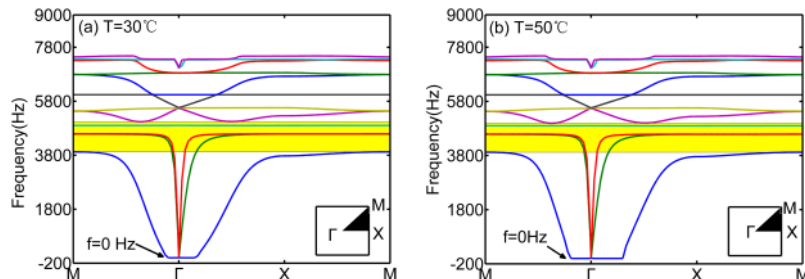
FIG. 7. Comparison of the band structures at room temperature and at 70°C while  $h=3\text{mm}$ .FIG. 8. Comparison of the band structures at room temperature and at 70°C while  $h=5\text{mm}$ .

FIG. 9. The vibration modal of the corresponding point denoted in FIG. 8. (a).

model with  $h=5\text{mm}$ . It is found that: (i) with temperature rising, the band gap moves to lower frequency since the structural vibration characteristics are affected by softening effect of the thermal stress on stiffness.<sup>23</sup> (ii) the width of flat band in the first flexure band is increased obviously with the temperature of 30°C, 50°C, 70°C, which corresponds to an increasing additional stress soften stiffness. (iii) except the emergence of zero-frequency flat band, the group velocity of the first flexure band increases with temperature, in which the definition of group velocity:<sup>24</sup>

$$v_g = \frac{d\omega}{dK} \quad (10)$$

where  $\omega$  is the frequency of elastic wave,  $K$  is the wave vector.

FIG. 10. The flat band in the lowest flexure band varies with different thermal stress state while  $h=5\text{mm}$ .



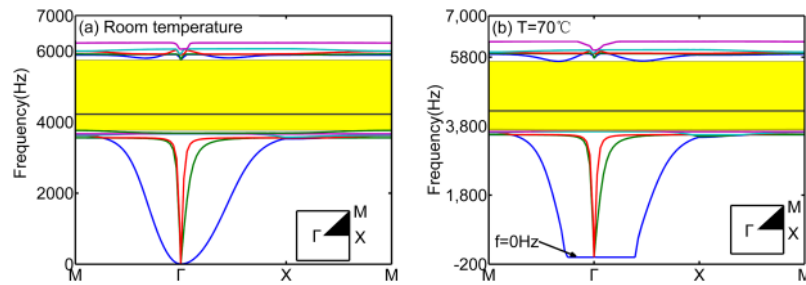


FIG. 11. Comparison of the band structure at room temperature and at 70°C while  $h=7\text{mm}$ .

As a result, based on the regular about the height of nitrile rubber effecting on band structure and its decrease trend in thermal environment, we can tune the band gap width and location by adjusting the height of nitrile rubber cylinder to obtain a proper gap in thermal environment.

#### IV. CONCLUSIONS AND OUTLOOK

In this paper, the influence of thermal stress on band gap variation trend and the band structure of created model is studied numerically. The regular of band gaps being narrower in thermal environment is obtained for the first time by taking thermal stress into consideration. Simulations show that the start and stop frequency of both flexure and complete band gaps shift to lower frequency as temperature increase. Moreover, the band gap (either flexure or complete band gap) is enlarged by changing the height of nitrile rubber. A proper band gap can be obtained in thermal environment via the research of the created model. The emergence of zero-frequency flat band in the first flexure band is fresh and deserved to further study.

As a new type of vibration and noise reduction material, acoustic metamaterial has a vast application prospect in engineering fields. Meanwhile, it is urgent to figure out its mechanic features so as to adapt multi physical environment. The regular of band gap width decreasing in thermal environment, as well as the wider band gap induced by the new model are helpful for PC structure to work in thermal environment. Ultimately, it is an inevitable challenge to take a further study about the deformation behavior of PC structure in thermal environment from both the macro and micro view.

#### ACKNOWLEDGMENTS

The authors gratefully acknowledge the financial support from the Natural Science Foundation of China (No. 11472206).

- <sup>1</sup> Z. Y. Liu, X. X. Zhang, Y. W. Mao *et al.*, *Science* **289**, 1734 (2000).
- <sup>2</sup> X. M. Zhou and G. K. Hu, *Phys. Rev. B* **79**, 195109-1 (2009).
- <sup>3</sup> X. M. Zhou and G. K. Hu, *Acta Mech.* **224**, 1233 (2013).
- <sup>4</sup> M. Hirsekorn, *Appl. Phys. Lett.* **84**, 3364 (2004).
- <sup>5</sup> R. Zhu, X. N. Liu *et al.*, *Phys. Rev. B* **25**, 144307 (2012).
- <sup>6</sup> M. Oudich, Y. Li *et al.*, *New J. Phys.* **12**, 083049 (2010).
- <sup>7</sup> M. Oudich, M. Senesi, M. B. Assouar *et al.*, *Phys. Rev.* **84**, 165136 (2011).
- <sup>8</sup> M. Oudich, B. Djafari-Rouhani *et al.*, *J. of Appl. Phys.* **11**, 184504 (2014).
- <sup>9</sup> J. C. Hsu and T. T. Wu, *Appl. Phys. Lett.* **90**, 201904 (2007).
- <sup>10</sup> J. C. Hsu and T. T. Wu, in *Proceeding of Symposium on Ultrasonic Electronics 18-20 November, 2009*, **30**, p. 449.
- <sup>11</sup> Q. Geng and Y. Li, *J. Acoust. Soc. Am.* **135**, 2674 (2014).
- <sup>12</sup> W. Li and Y. M. Li, *Acta Mechanica Solida Sinica*, **28**, 11 (2015).
- <sup>13</sup> Y. Liu and Y. M. Li, *Shock Vib.* **20**, 1011 (2013).
- <sup>14</sup> P. Wang, T. N. Chen, K. P. Yu *et al.*, *J. Appl. Phys.* **113**, 053509 (2013).
- <sup>15</sup> Y. Yao, F. Wu, X. Zhang, and Z. Hou, *J. Appl. Phys.* **110**, 123503 (2011).
- <sup>16</sup> D. Flight, M. W. Kehoe, and V. C. Deaton, NASA Technical Memorandum, **104269**, 1 (1993).
- <sup>17</sup> R. D. Cook, D. S. Malkus, M. E. Plesha *et al.* (Wiley, New York, 1989) p. 429.
- <sup>18</sup> Y. Cheng, X. J. Liu, and D. J. Wu, *J. Acoust. Soc. Am.* **129**, 1157 (2011).
- <sup>19</sup> K. L. Jim, C. W. Leung, S. T. Lau *et al.*, *Appl. Phys. Lett.* **94**, 193501 (2009).
- <sup>20</sup> A. Anthoine, *Int. J. Solids Structures*, **32**, 137 (1995).

- <sup>21</sup> COMSOL MULTIPHYSICS 5.0 Manual, User's Guide of Structural Mechanics Module, Thermal-Structure Interaction Section.
- <sup>22</sup> M. R. Eslami, R. B. Hetnarski, G. M. L. Gladwell (Springer, New York, 2009) p. 22.
- <sup>23</sup> M. Du, Q. Geng, and Y. M. Li, [Compos. Struct.](#) **157**, 483 (2016).
- <sup>24</sup> C. Kittel, 6th Ed (Wiley & Sons, New York, 1986) p. 86.